

Electronic Supplementary Information

A novel characteristic of salicylate UV absorbers: suppression of diethylhexyl 2,6-naphthalate (Corapan TQ)-photosensitized singlet oxygen generation

Shirabe Fukuchi ^a, Mikio Yagi ^{a*}, Nozomi Oguchi-Fujiyama ^b, Jasmin Kang ^b, Azusa Kikuchi ^{a*}

^a Department of Chemistry, Graduate School of Engineering Science, Yokohama National University, Tokiwadai, Hodogaya-ku, Yokohama 240-8501, Japan.

^b Shiseido Global Innovation Center, Hayabuchi, Tsuzuki-ku, Yokohama 224-8558, Japan.

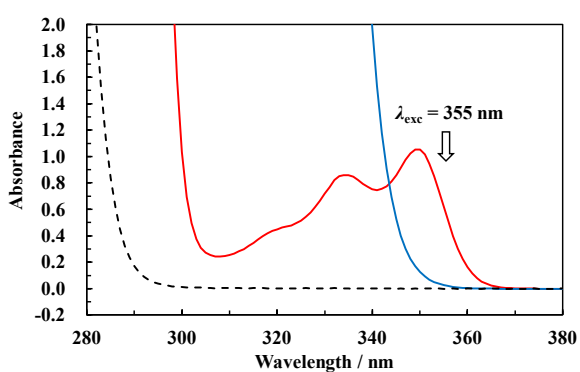


Fig. S1 UV absorption spectra of (a) DEHN (0.4 mmol dm⁻³, red), (b) HMS (32 mmol dm⁻³, blue) and (c) 3-EtAA (32 mmol dm⁻³, broken line) in ethanol at 25 °C.

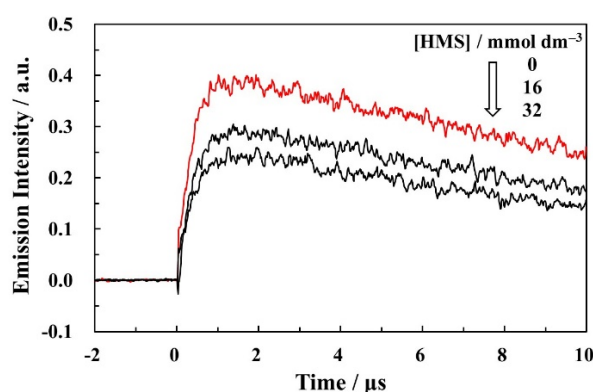


Fig. S2 Kinetic traces of the phosphorescence intensity of singlet oxygen taken following 355 nm laser excitation of DEHN (0.4 mmol dm⁻³) in air-saturated ethanol at 25 °C in the absence (red) and presence of HMS. The phosphorescence intensity was monitored at 1274 nm.

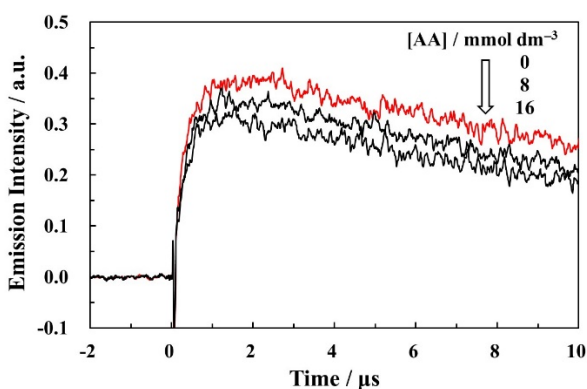


Fig. S3 Kinetic traces of the phosphorescence intensity of singlet oxygen taken following 355 nm laser excitation of DEHN (0.4 mmol dm⁻³) in air-saturated ethanol at 25 °C in the absence (red) and presence of AA. The phosphorescence intensity was monitored at 1274 nm.

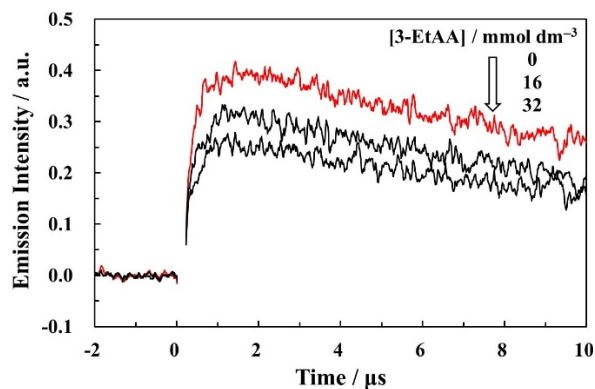


Fig. S4 Kinetic traces of the phosphorescence intensity of singlet oxygen taken following 355 nm laser excitation of DEHN (0.4 mmol dm⁻³) in air-saturated ethanol at 25 °C in the absence (red) and presence of 3-EtAA. The phosphorescence intensity was monitored at 1274 nm.

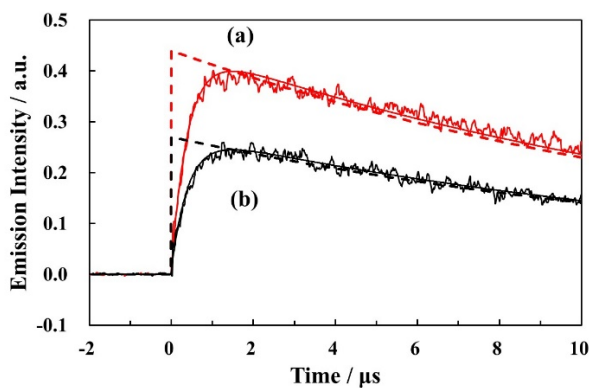


Fig. S5 Kinetic traces of the phosphorescence intensity of singlet oxygen generated by excitation of DEHN (0.4 mmol dm^{-3}) (a) in the absence (red) and (b) presence of HMS (32 mmol dm^{-3}) in air-saturated ethanol at $25 \text{ }^\circ\text{C}$. Computer-simulated kinetic traces obtained with (a) $c = 1.0$, $\Phi_{\Delta} = 0.44$, $\tau_{\Delta} = 15.4 \text{ } \mu\text{s}$, $\tau_{\text{T}} = 0.001 \text{ } \mu\text{s}$ (broken line) and $\tau_{\text{T}} = 0.40 \text{ } \mu\text{s}$ (solid line), and (b) $c = 1.0$, $\Phi_{\Delta} = 0.27$, $\tau_{\Delta} = 15.4 \text{ } \mu\text{s}$, $\tau_{\text{T}} = 0.001 \text{ } \mu\text{s}$ (broken line) and $\tau_{\text{T}} = 0.40 \text{ } \mu\text{s}$ (solid line).

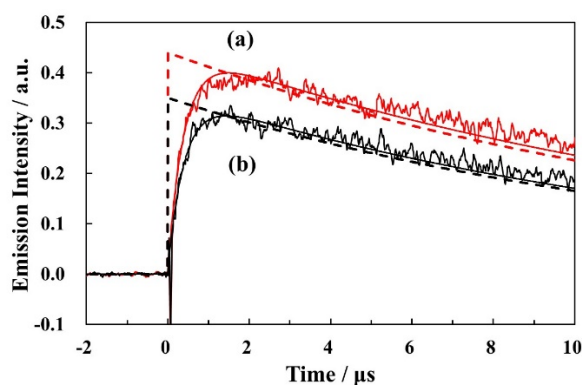


Fig. S6 Kinetic traces of the phosphorescence intensity of singlet oxygen generated by excitation of DEHN (0.4 mmol dm^{-3}) (a) in the absence (red) and (b) presence of AA (16 mmol dm^{-3}) in air-saturated ethanol at $25 \text{ }^\circ\text{C}$. Computer-simulated kinetic traces obtained with (a) $c = 1.0$, $\Phi_{\Delta} = 0.44$, $\tau_{\Delta} = 15.4 \text{ } \mu\text{s}$, $\tau_{\text{T}} = 0.001 \text{ } \mu\text{s}$ (broken line) and $\tau_{\text{T}} = 0.40 \text{ } \mu\text{s}$ (solid line), and (b) $c = 1.0$, $\Phi_{\Delta} = 0.35$, $\tau_{\Delta} = 13.3 \text{ } \mu\text{s}$, $\tau_{\text{T}} = 0.001 \text{ } \mu\text{s}$ (broken line) and $\tau_{\text{T}} = 0.40 \text{ } \mu\text{s}$ (solid line).

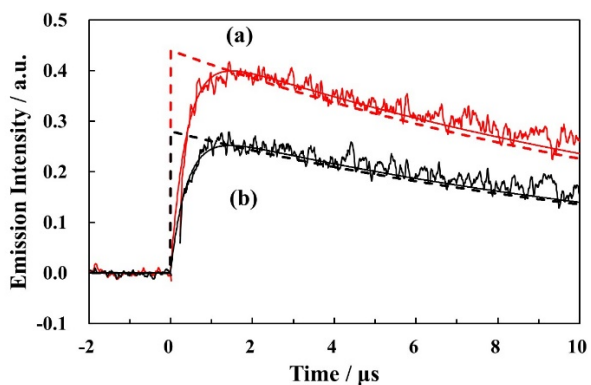


Fig. S7 Kinetic traces of the phosphorescence intensity of singlet oxygen generated by excitation of DEHN (0.4 mmol dm^{-3}) (a) in the absence (red) and (b) presence of 3-EtAA (32 mmol dm^{-3}) in air-saturated ethanol at $25 \text{ }^\circ\text{C}$. Computer-simulated kinetic traces obtained with (a) $c = 1.0$, $\Phi_{\Delta} = 0.44$, $\tau_{\Delta} = 15.4 \text{ } \mu\text{s}$, $\tau_{\text{T}} = 0.001 \text{ } \mu\text{s}$ (broken line) and $\tau_{\text{T}} = 0.40 \text{ } \mu\text{s}$ (solid line), and (b) $c = 1.0$, $\Phi_{\Delta} = 0.28$, $\tau_{\Delta} = 13.8 \text{ } \mu\text{s}$, $\tau_{\text{T}} = 0.001 \text{ } \mu\text{s}$ (broken line) and $\tau_{\text{T}} = 0.40 \text{ } \mu\text{s}$ (solid line).

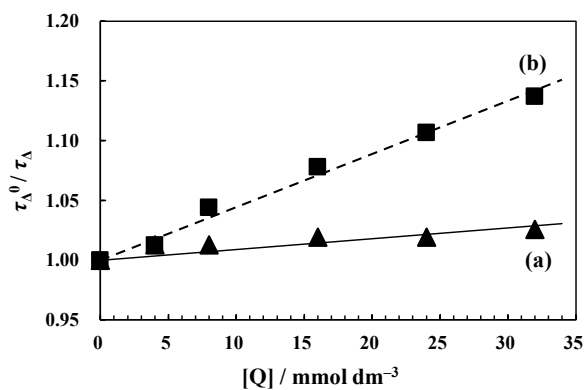


Fig. S8 Stern-Volmer plots according to Eq. (3) for the quenching of singlet oxygen by (a) HMS and (b) 3-EtAA in ethanol at $25 \text{ }^\circ\text{C}$.

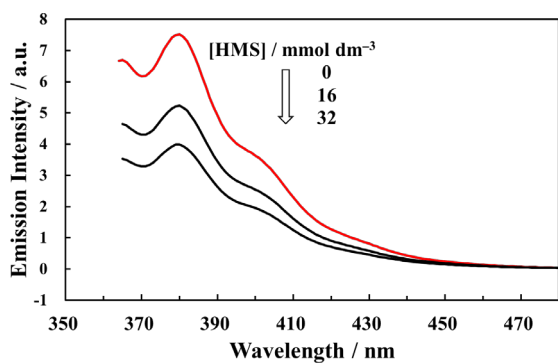


Fig. S9 Fluorescence ($\lambda_{\text{ex}} = 355 \text{ nm}$) spectra of DEHN in the absence (red) and presence of HMS in air-saturated ethanol at $25 \text{ }^\circ\text{C}$.

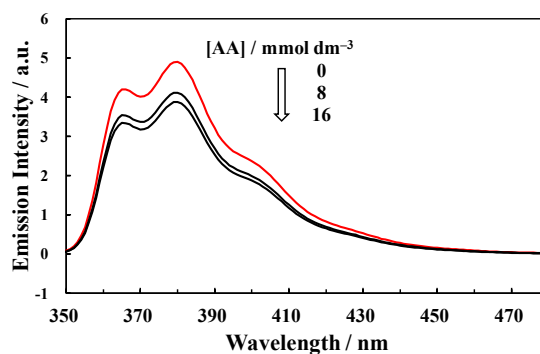


Fig. S10 Fluorescence ($\lambda_{\text{ex}} = 334 \text{ nm}$) spectra of DEHN in the absence (red) and presence of AA in air-saturated ethanol at $25 \text{ }^\circ\text{C}$.

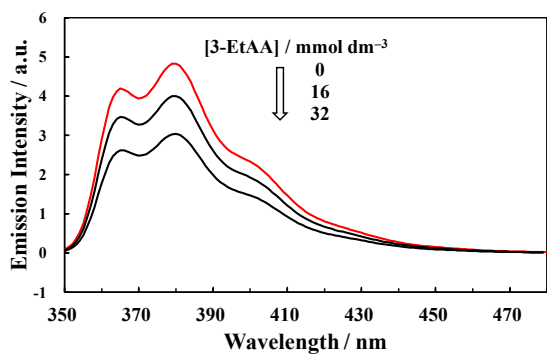


Fig. S11 Fluorescence ($\lambda_{\text{ex}} = 334 \text{ nm}$) spectra of DEHN in the absence (red) and presence of 3-EtAA in air-saturated ethanol at 25 °C.

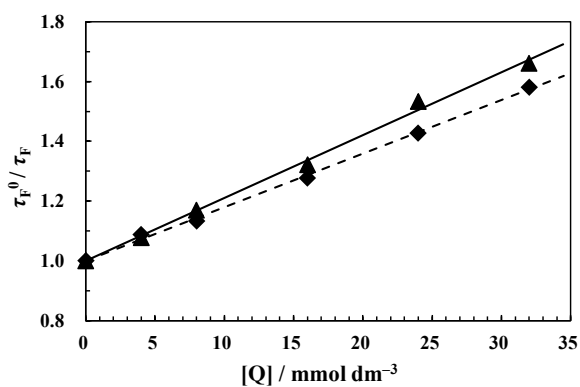


Fig. S12 Stern–Volmer plots according to Eq. (5) for the quenching of the S₁ state of DEHN by HMS (solid line) and 3-EtAA (broken line) in air-saturated ethanol at 25 °C. Emissions were monitored at 380 nm.

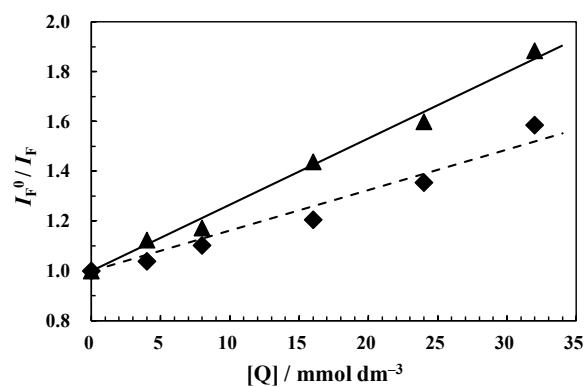


Fig. S13 Stern–Volmer plots according to Eq. (6) for the quenching of the S₁ state of DEHN by HMS (solid line) and 3-EtAA (broken line) in air-saturated ethanol at 25 °C. Emissions were monitored at 380 nm.

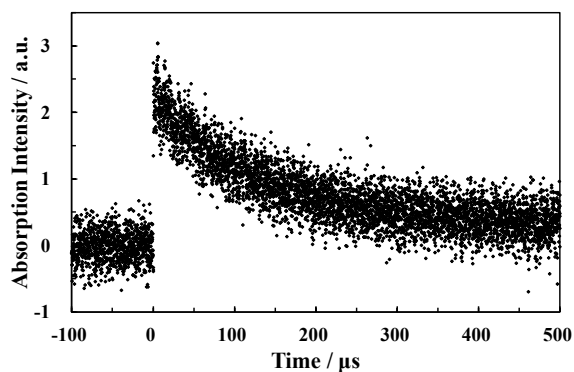


Fig. S14 Kinetic trace of the transient absorption following 355 nm laser excitation of DEHN (4.1 mmol dm⁻³) in degassed ethanol at 25 °C. The transient absorption was monitored at 510 nm.